Ultrasonics Sonochemistry 79 (2021) 105797

Contents lists available at ScienceDirect

Ultrasonics Sonochemistry

journal homepage: www.elsevier.com/locate/ultson

Study of double-using ultrasonic effects on the structure of PbO nanorods fabricated by the sonochemical method

Sepideh Yazdani-Darki, Mohammad Eslami-Kalantari *, Hakimeh Zare

Physics Department, Faculty of Science, Yazd University, Yazd, P.O.Box 89195-714, Iran

ARTICLE INFO

Keywords:
Sonochemical method
Re-ultrasonic effect
PbO nanorod
Calcination time

ABSTRACT

In this study, lead oxide (PbO) nanostructures are fabricated by an ultrasound-assisted sonochemical method, and re-ultrasonic effects on them are investigated. In the synthesis process, lead nitrate powder is used as a precursor, and potassium hydroxide serves as a precipitation agent. The resulting samples are characterized by scanning electron microscopy (SEM), X-ray diffraction (XRD), energy-dispersive X-ray spectroscopy (EDX), and Fourier transform-infrared spectroscopy (FT-IR). Re-ultrasound is also performed to terminate the growth of the PbO nanorods, stabilize them, and preserve their morphology. According to the XRD results, the re-ultrasonic effect did not change the crystal phases, and the tetragonal and orthorhombic crystal phases were preserved. The effect of the calcination time was investigated too; an increase in it led to a decrease in the irregular nanorods size but an increase in the crystallite size.

1. Introduction

Lead oxide nanostructures are important metal oxide nanomaterials [1]. In recent decades, extensive research has been done on the fabrication and application of these nanostructures. They have unique physical and chemical properties such as a high surface area-to-volume ratio and excellent reactivity to bulk materials [2]. They have also been used for various industrial and medical purposes, as in fabricating optoelectronic devices [3], solar cells [4], and batteries [5]. The high atomic number of lead oxide makes it appropriate for the attenuation of × and gamma rays in medicine [1,6]. However, it is not without disadvantages. For example, as a protector against ionizing radiation, it is too dense. The use of lead oxide nanostructures is a solution to this problem. These materials are comparable to those used in some electrochemical systems, as in batteries [7,8]. With their good ability to absorb visible light, lead oxide nanomaterials are widely used in solar cells [9]. Furthermore, due to the high density and refractive index of lead oxide, its nanomaterials are used in the glass industry to reduce the effect of ultraviolet radiation [10].

Lead oxide nanostructures have four distinct semiconducting oxide forms, namely PbO, PbO_2, Pb_2O_3, and Pb_3O_4. Among them, PbO possesses unique electronic, mechanical, and optical features, thus favored in nanodevices that can be crystallized in α and β phases [11]; α-PbO (tetragonal phase or litharge) is stable at low temperatures and red in color, while β-PbO (orthorhombic phase or massicot) is stable at high temperatures and yellow in color [12,13].

Controlling the growth of PbO nanostructures is essential for their application in various fields [14,15]. Recently, several routes have been taken to synthesize PbO nanostructures, such as sonochemical method [7,16], sol–gel combustion [17], anodic oxidation [18], spray pyrolysis [19], electrodeposition and electrochemistry [20,21], hydrothermal method [22], and thermal decomposition [23].

It has been proved that the particle size of nanomaterials, like their other properties, depends on the method of preparation and the experimental conditions applied. Currently, the sonochemical method is in common use to produce nanomaterials because it can form particles of a much smaller size and a larger surface area than those reported by other methods [24–29]. The sonochemical method is a convenient, economical, and fast way to synthesis nanomaterials. Ultrasound is a sound wave in the frequency range of 20 kHz to 10 MHz [30–34]. Ultrasonic waves affect nanomaterials by reducing their particle size and preventing their agglomeration. In addition, an increase in the calcining time causes a change in the particle size [29,35–37]. So far, few studies have been reported on the sonochemical synthesis of lead oxide nanostructures. Yazdani et al. [38] used ultrasonic waves to synthesize PbO nano and microstructures by a simple precipitation method. The samples were synthesized using various alkalis as precursors and polyvinyl pyrrolidone as a surfactant. The results showed that alkaline factors can

* Corresponding author.
E-mail address: meslami@yazd.ac.ir (M. Eslami-Kalantari).

https://doi.org/10.1016/j.ultsonch.2021.105797
Received 14 July 2020; Received in revised form 23 September 2021; Accepted 14 October 2021
Available online 15 October 2021

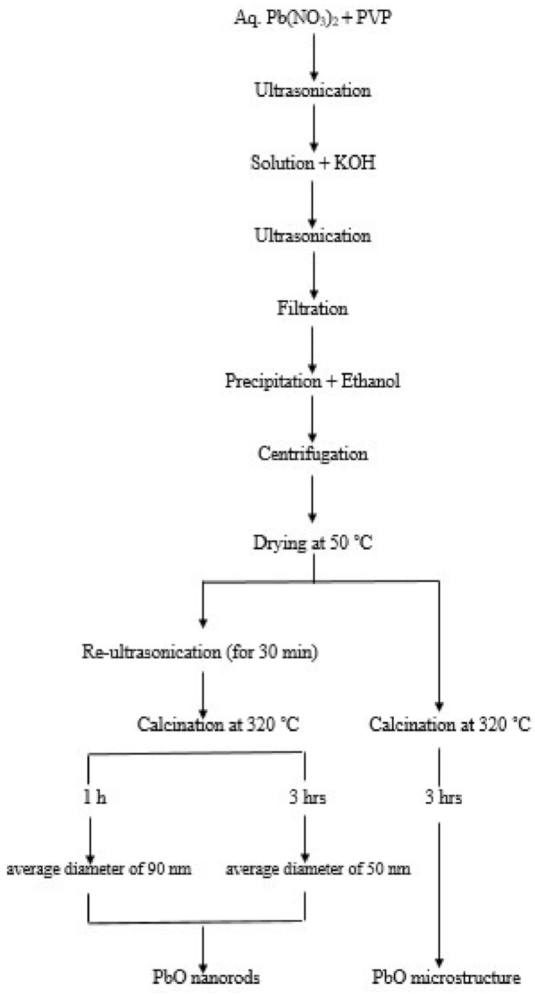

Fig. 1. Flowchart for the synthesis of PbO microstructures/nanorods by a sonochemical method.

create different structures and the presence of a surfactant can also help to form small particulates and more regular shapes in PbO nanostructures. Karami et al. [7] synthesized PbO nanoparticles by a sonochemical method through the reaction of lead nitrate and a sodium hydroxide solution. They used constant-frequency ultrasonic waves to prepare agglomerated nanoparticles with the size of 20–40 nm. Ghasemi et al. [39] synthesized PbO_2 nanopowder by the ultrasonication of an aqueous β-PbO microstructure suspension. The resulting samples of PbO_2 were agglomerated nanoparticles in the range of 50–100 nm in size. Bangi et al. [40] synthesized PbO nanoflowers using several ligands. They prepared their samples by ultrasonic and ball milling techniques. The final products were nanodiscs and nanoflowers with a diameter of around 300 nm and thickness of 50 nm.

Investigating the effects of ultrasonic waves on the structure and physical properties of materials can be interesting. For instance, the effects of these waves on fabrication processes as well as post-fabrication stages determine the material morphology in the field of nanotechnology. There is no report about re-ultrasonic effects on PbO structures. The present study, however, is dedicated to the effects of re-ultrasonication on the morphology and the particle size of PbO structures. In this study, PbO nanorods are synthesized with a simple sonochemical method using inexpensive precursors and biocompatible solvents within a short time and at a low temperature. Then, the effects of re-ultrasonication and calcination time on the morphology and the crystal structure of the final products are evaluated through scanning electron microscopy (SEM) and X-ray diffraction (XRD), energy-dispersive X-ray (EDX) and fourier transform infrared (FT-IR) techniques.

2. Materials and methods

2.1. Materials

All the chemicals were commercially available and used without further purification. Lead nitrate ($Pb(NO_3)_2$, 99 %), polyvinyl pyrrolidone (PVP, 98 %), potassium hydroxide (KOH, 90 %), and ethanol (96 %) as a solvent were purchased from Merck.

2.2. Characterization

In this study, an FT-IR spectrometer (Equinox 55, Germany) was employed to identify the functional groups of the synthesized nanomaterial samples. The samples were mixed with KBr at the ratio of 1:20 to fabricate pellets for recording the FTIR spectra. An SEM (Vega3 Tescan, Czech Republic, 15 kV) was also used to view the structure and the quality of the samples. To prepare the samples for this analysis, they were coated with a 15-nm layer of Au. The crystal structure of the nanostructures was studied by means of an X-ray diffractometer with CuKα radiation (X'PertPro, Philips X'Pert, the Netherlands, $\lambda = 1.5418$ Å). Finally, the purity of the samples was determined with an EDX spectroscope (TESCAN XMU VEGA, Czech Republic).

2.3. Synthesis procedure

Lead nitrate ($Pb(NO_3)_2$), KOH, PVP, Ethanol, and distilled water were used to synthesize PbO nanostructures. First, 1.32 g of $Pb(NO_3)_2$, and 0.008 mol of KOH were dissolved in 100 ml of distilled water separately, and the solution was stirred to obtain a clear one. Then, PVP (20 g/mol), as a surfactant, was added to the $Pb(NO_3)_2$ solution. They were stirred for 20 min until the PVP was completely dissolved in it. A surfactant plays a significant role to prevent agglomeration and obtain finer structures [21]. The $Pb(NO_3)_2$ and the PVP solution were ultrasonicated for 30 min at the temperature of 40 °C. Next, the KOH solution (pH ≈ 12) was added drop-wise to the solution of the lead salt and the surfactant on the stirrer. They were mixed thoroughly by a stirring apparatus at room temperature (28 °C) for 5 min.

The reaction for nanostructured lead hydroxide is as follow:

$$Pb(NO_3)_2(aq) + 2KOH(aq)\ Pb(OH)_2(s) + 2KNO_3(aq) \quad (1)$$

In the next step, the resulting solution was ultrasonicated for 30 min at 40 °C. The obtained precipitate was first filtered and then washed with distilled water and ethanol for three times. After the precipitation was filtered, it was dissolved in 50 ml of ethanol, and the mixture underwent ultrasonic waves at 40 °C for 30 min. Then, the precipitation was dried at 50 °C for eight hours. From now on, this procedure will be referred to as L1. Finally, the final product was calcined at 320 °C for three hours. This process will be referred to as L2. Reaction (2) represents the L2 process.

$$Pb(OH)_2(s)PbO(s) + H_2O(g) \quad (2)$$

At the end of the synthesis of sample L1, first, the powder was dissolved in 20 ml of an ethanol solution, and then the precipitate was filtered to be lastly washed with distilled water and ethanol three times. After filtration, the obtained precipitation was dissolved in 50 ml of ethanol, and the resulting solution was exposed to ultrasonication for 30 min at the temperature of 40 °C. This process led to a new precipitation which was dried at 50 °C for eight hours. The final product was divided into two parts. They were calcined at 320 °C for one hour (sample L3) and three hours (sample L4).

Fig. 1 presents the flowchart of the synthesis method. The main reactions occurring during the experimental procedure can by written

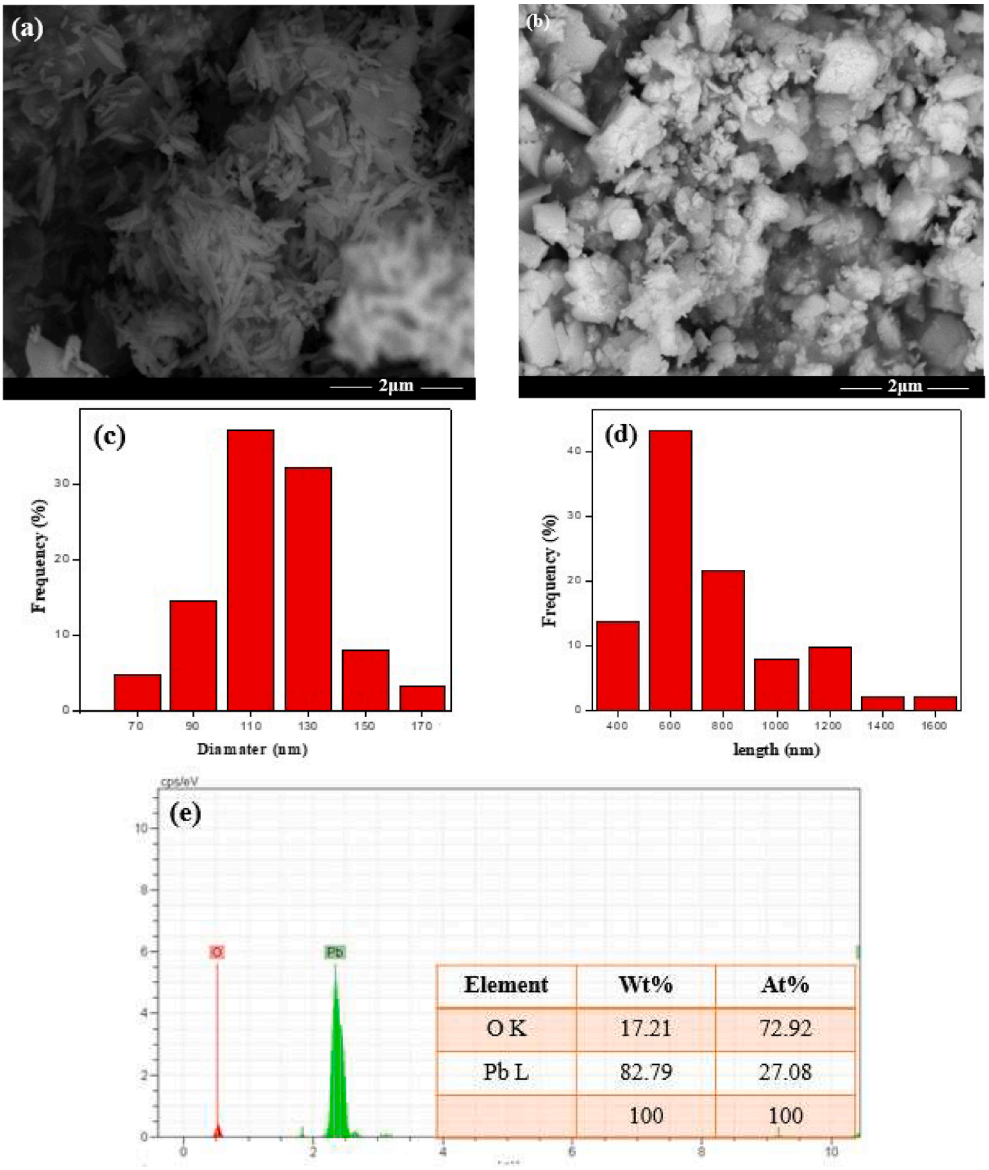

Fig. 2. The SEM image (a), the diameter and length histogram frequency chart of L1 (c and d), the SEM image (b), and the EDX spectrum of L2 (e).

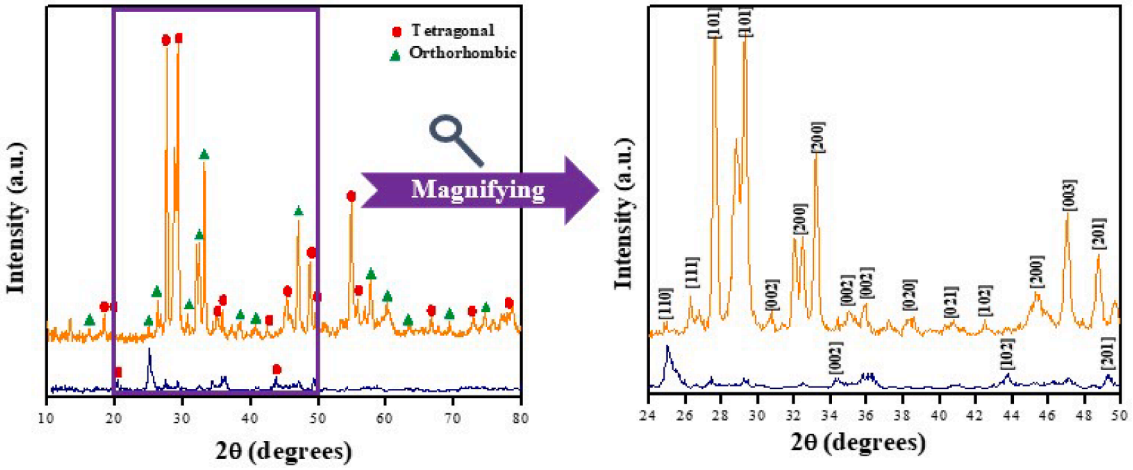

Fig. 3. XRD patterns of the nano and microstructures obtained for samples L1 (Royal) and L2 (Orange). (For interpretation of the references to color in this figure legend, the reader is referred to the web version of this article.)

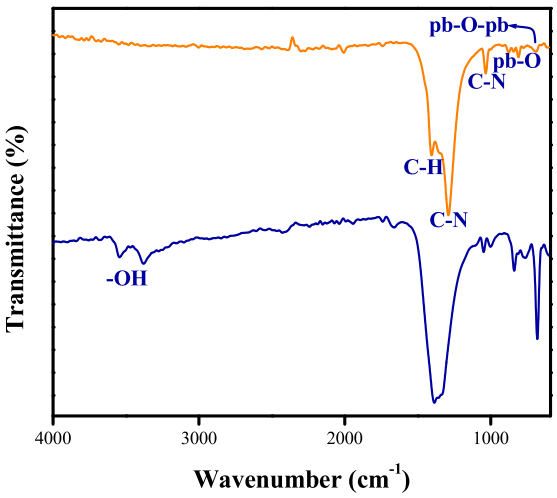

Fig. 4. FT-IR spectra of PbO nano and microstructures for samples L1 (Royal) and L2 (Orange). (For interpretation of the references to color in this figure legend, the reader is referred to the web version of this article.)

briefly as follows:

The process of water sonolysis is as follows [41]:

$$H_2O \rightarrow {}^{\circ}H + {}^{\circ}OH \quad (3)$$

$${}^{\circ}OH + {}^{\circ}OH \rightarrow H_2O \quad (4)$$

$${}^{\circ}OH + {}^{\circ}OH \rightarrow H_2 + O_2 \quad (5)$$

$${}^{\circ}H + O_2 \rightarrow {}^{\circ}H_2O \quad (6)$$

$${}^{\circ}H_2O + {}^{\circ}H \rightarrow H_2O_2 \quad (7)$$

$${}^{\circ}H_2O + {}^{\circ}H_2O \rightarrow H_2O_2 + O_2 \quad (8)$$

$${}^{\circ}OH + H_2O \rightarrow H_2O_2 + {}^{\circ}O \quad (9)$$

$${}^{\circ}H + {}^{\circ}H \rightarrow H_2 \quad (10)$$

$${}^{\circ}H + {}^{\circ}OH \rightarrow H_2O_2 \quad (11)$$

The formation of metal oxides by the sonochemical method occurs through the following process:

$$Pb(NO_3)_2 \rightarrow Pb^{+2} + 2NO_3^- \quad (12)$$

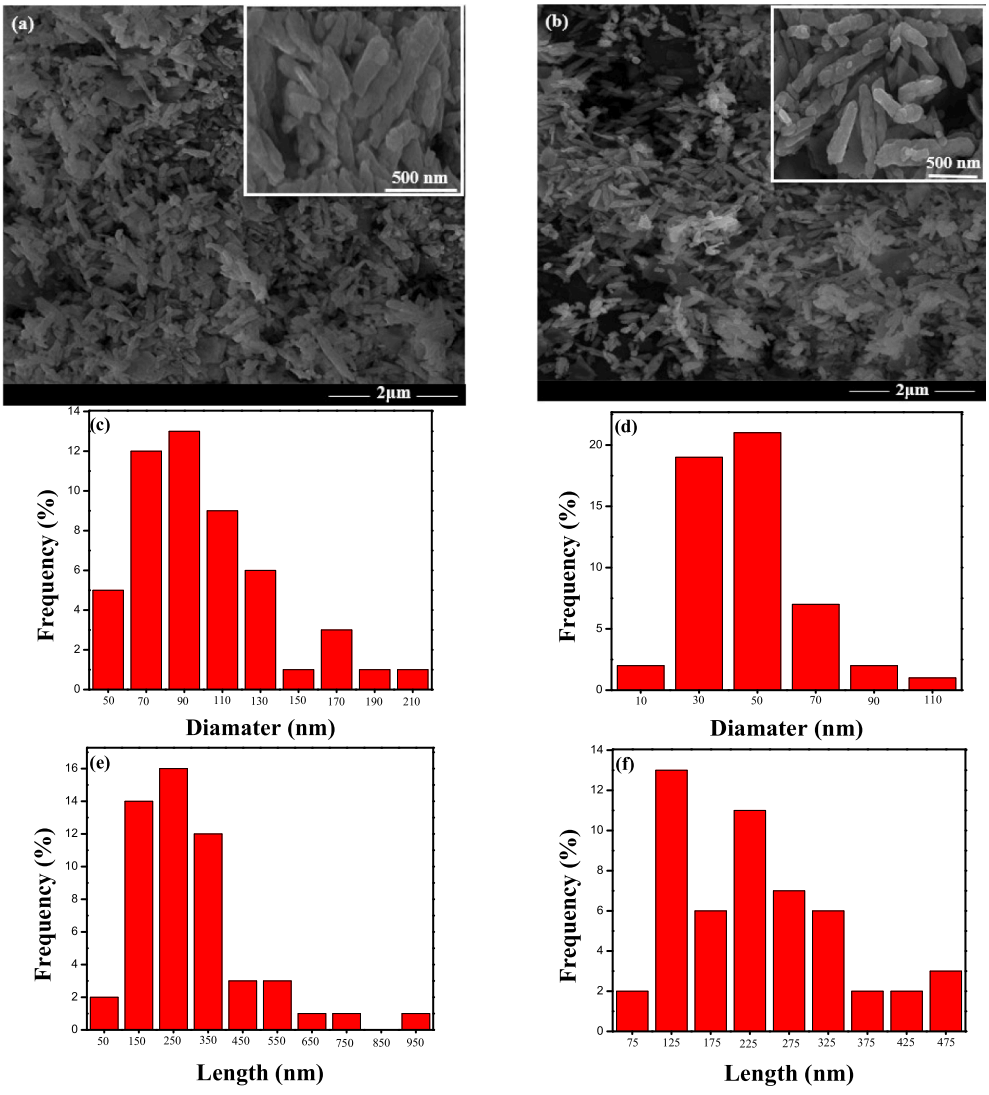

Fig. 5. The SEM images of L3 and L4 samples (a and b), diameter (c and d) and length histogram frequency charts (e and f) of L3 and L4 samples, respectively.

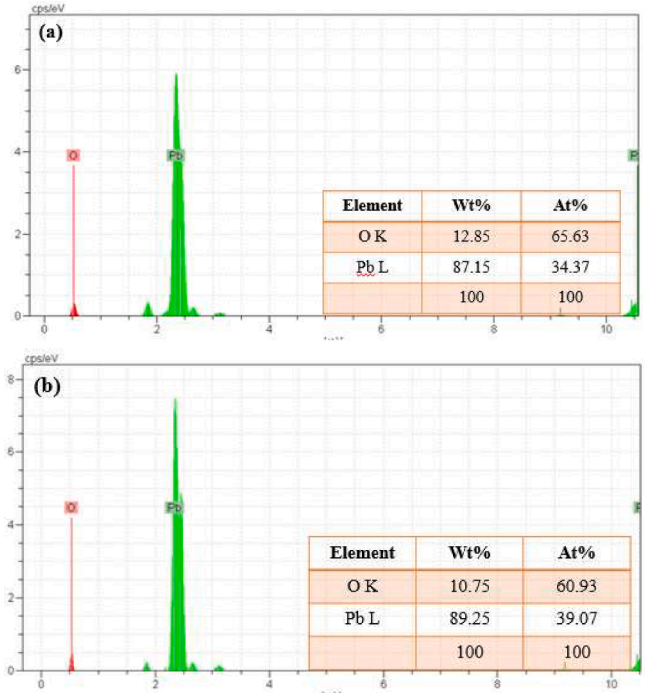

Fig. 6. The EDX spectra of L3 and L4 samples (a and b).

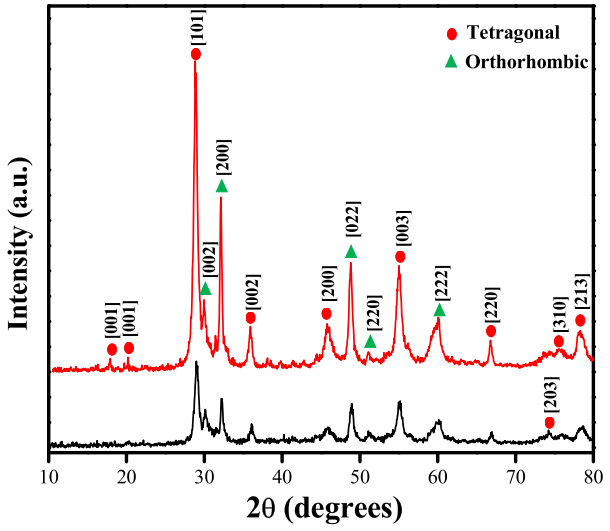

Fig. 7. XRD patterns of the nanostructures obtained during one hour (Black) and three hours (Red) of re-ultrasonication and calcination. (For interpretation of the references to color in this figure legend, the reader is referred to the web version of this article.)

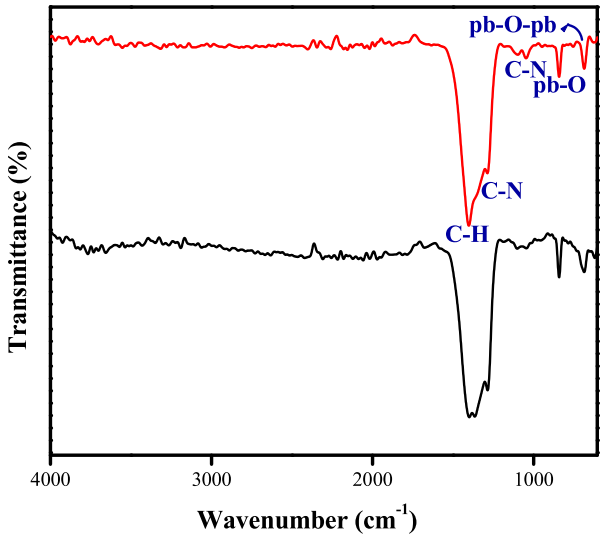

Fig. 8. FT-IR spectra of re-ultrasonication (30 min) and calcination for one hour, L3 (black), and three hours, L4 (red). (For interpretation of the references to color in this figure legend, the reader is referred to the web version of this article.)

$$KOH \rightarrow K^{+} + OH^{-} \quad (13)$$

$$Pb^{+2} + 2\,^{\circ}OH \rightarrow PbO_2 + 2\,^{\circ}H \quad (14)$$

$$PbO_2 + 2OH^{-} + 2H_2O \rightarrow Pb(OH)_6^{-2} \quad (15)$$

$$Pb(OH)_6^{-2} \rightarrow Pb^{+4} + 6OH^{-} \quad (16)$$

$$Pb^{+4} + H_2O_2 \rightarrow Pb^{+2} + H^{+} + {}^{\circ}H_2O \quad (17)$$

$$Pb^{+2} + 2OH^{-} \rightarrow Pb(OH)_2 \quad (18)$$

$$2H^{+} \rightarrow H_2 \quad (19)$$

$$^{\circ}H_2O + {}^{\circ}H_2O \rightarrow {}^{\circ}H_2O_2 + {}^{\circ}O_2 \quad (20)$$

3. Results and discussion

3.1. Characterization of the PbO nano/micro structure

This study sought to evaluate the effect re-ultrasonication on the size and the morphology of the PbO structure. Fig. 2 shows the morphologies and the elemental characteristics of PbO before and after calcination at 320 °C (L1 and L2 samples). The sample before calcination was like a nanorod (Fig. 2a) 600 nm in length and 110 nm in diameter. Fig. 2b clearly shows that nano and microstructures with the sizes of 40 nm and 1 μm grew in the calcination process. The EDX spectrum show that the sample was composed of Pb (82.79 %) and O (17.21 %) elements and there were no any impurities in the sample.

Fig. 3 shows the XRD patterns of the synthesized samples L1 and L2. The data were collected at room temperature in the 2θ range of 10-80°. The average crystallite size of the PbO nanoparticles was calculated using the Debye-Scherrer formula as follows [42]:

$$D = \frac{0.9\lambda}{\beta \cos\theta} \quad (21)$$

where D is the mean crystallite size, λ stands for the wavelength of the CuKα line (=1.5405 Å), β represents the full width at half maximum (FWHM), and θ is the Bragg's diffraction angle. According to Fig. 3, there are two different phases of PbO in the patterns. To have a clearer view, a

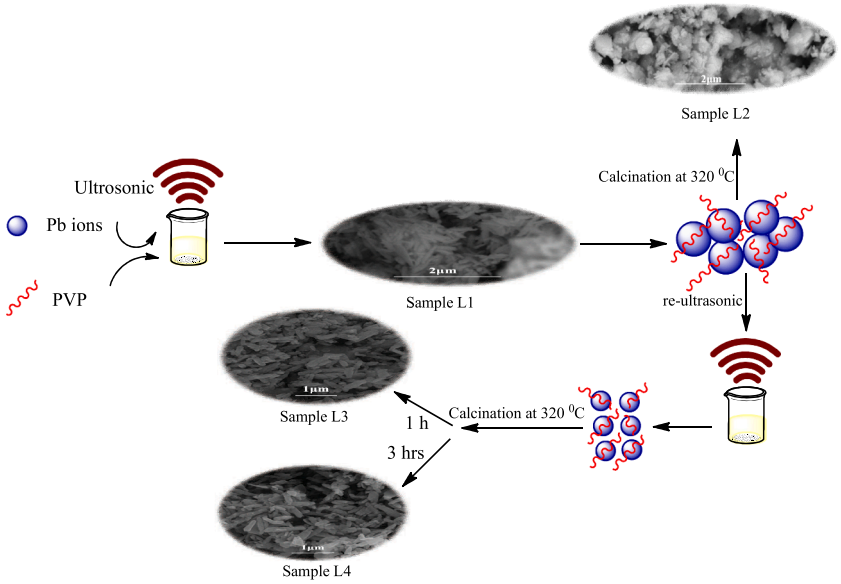

Fig. 9. Schematic illustration of the synthesis of PbO nanorods by a re-ultrasonic precipitation process.

magnified image of the patterns from 24° to 50° is provided on the right of the figure. The results showed that, in sample L1, the tetragonal phase of PbO (Ref. code: 00–001-0796) was the most crystallite-like structure. In the sample prepared at a higher temperature, however, the majority of the structures had an orthorhombic form (Ref. code: 00–003-0599). There were also some additional peaks, which were attributed to the tetragonal (Ref. code: 00–001-0824) and orthorhombic (Ref. code: 00–003-0600) structures. Sample L2 was crystallized in tetragonal and orthorhombic phases. The average size of the crystallite in samples L1 and L2 was about 24.2 nm and 31 nm, respectively. It is concluded that the calcining process can lead to the growth of crystallites.

The PVP surfactant in PbO organizes nanostructures by forming a cation-PVP complex, which also moderates the crystal growth rate and makes oriented nuclei leading to the anisotropic growth of the nanostructures. The bonding of PVP occurs through both nitrogen (N) and oxygen (O) ions. Therefore, the surfactant has a significant effect on the shape and the size of the structure; it plays a vital role in the formation of nanostructures [38]. FT-IR spectra were used to analyze the vibrations of the functional groups existing in the samples. Fig. 4 shows the FT-IR transmission spectra of samples L1 and L2 in the range of 500–4000 cm^{-1}. In sample L1, the vibration band at 3660–3380 cm^{-1} was related to –OH, which suggests the existence of H_2O in the sample; it was removed after calcining L2. The rest of the FT-IR transmission spectra are totally the same for samples L1 and L2, but the samples are not identical in terms of vibration band intensity. The peaks of PVP could be observed at 1200–1500 cm^{-1}. They were related to the C-N group [43] and the modes of C − H deformation from the CH_2 groups [43–45]. In addition, the bending of Pb-O and pb-O-pb chains were associated with the bands at 650–1000 cm^{-1} [12].

3.2. Effects of re-ultrasonication and calcination duration

As Fig. 2 shows, after calcination, the nanorod structure was destroyed completely and an agglomerated micro-structure appeared. To preserve the nanoscale structure, sample L1 was ultrasonicated for 30 min and then calcined at 320 °C for one hour (L3 as in Fig. 5a) and three hours (L4 as in Fig. 5b). Fig. 5 shows the effects of re-ultrasonication and calcination time on the particle size of PbO. As it can be seen in Fig. 5c and 5e, the nanorods that underwent an hour of calcination had an average diameter of 90 nm and a length of 250 nm. Micrometric particles are presented in Fig. 5a; they look relatively small. As in Fig. 5d and 5f, the average diameter of the nanorods was about 50 nm, and the particle length was about 125 nm. There were, however, no micrometric particles. The calcination time also reduced the average particle size. Moreover, the EDX spectra of the sample showed that only Pb and O had no impurities (Fig. 6a and 6b). EDX indicated that the calcined PbO nanorods contained 100 % PbO. Also, compared to the sample without re-ultrasound (L2 sample), L3 and L4 samples under re-ultrasound showed decreased oxygen and increased lead.

Fig. 7 shows the XRD patterns of the PbO synthesized through the re-ultrasonication and calcination of L3 for one hour and L4 for three hours. Tetragonal and orthorhombic PbO structures were obtained after one and three hours of calcination. As the calcination time increased, the process led to the growth of crystallite size from 20.3 nm to 25.3 nm. A comparison of the crystallite size and the SEM images showed that the resulting samples were crystalized into a polycrystalline structure. Furthermore, a comparison of the ultrasonicated and the re-ultrasonicated results, i.e., L2 and L4, showed that re-ultrasonication could decrease the crystallite size from 31 nm to 25.3 nm, whereas no change occurred in the type of the crystal phase.

Fig. 8 shows the FT-IR transmission spectra of re-ultrasonication and calcination for one and three hours. As it can be seen, the FT-IR spectra of samples L3 and L4 are similar. Fig. 9 presents the schematic illustration of the synthesis method. Re-ultrasonication had a great influence on the structure of PbO such that nanorods were obtained as a final structure. Therefore, the re-ultrasonication method can be used to maintain the initial shape of particles and reduce their size.

4. Conclusion

PbO nanorods were successfully synthesized with a combination of a sonochemical method and re-ultrasonication. As the results showed, re-ultrasonic treatment is an efficient method of terminating the growth of PbO and stabilizing it. The functional groups, structural properties, and morphology of PbO nanorods were thoroughly studied. The crystallite size of the nanorods calculated by Debye-Scherrer formula using XRD pattern was about 20–25 nm. Their crystallinity was found to increase under the effect of re-ultrasound. The SEM images indicated that re-ultrasonication has a significant effect on the morphology of PbO. The average particle size of the sample L2 was 1 μm, but the average diameter sizes of the nanorods in the samples L3 and L4 were 90, and 50 nm. Thus, as a defendable conclusion, the re-ultrasonication method can be used to reduce the size of particles without changing their initial morphology.

Declaration of Competing Interest

The authors declare that they have no known competing financial interests or personal relationships that could have appeared to influence the work reported in this paper.

References

[1] H.O. Tekin, E. Kavaz, M. Athanasia Papachristodoulou, O.A. Kamislioglu, E. E. Altunsoy Guclu, O. Kilicoglu, M.I. Sayyed, Characterization of SiO_2–PbO–CdO–Ga_2O_3 glasses for comprehensive nuclear shielding performance: alpha, proton, gamma, neutron radiation, Ceram. Int. (2019), https://doi.org/10.1016/j.ceramint.2019.06.168.

[2] A. Hamid, M. Khan, A. Hayat, J. Raza, A. Zada, A. Ullah, F. Raziq, T. Li, F. Hussain, Probing the physio-chemical appraisal of green synthesized PbO nanoparticles in PbO-PVC nanocomposite polymer membranes, Spectrochim. Acta Part A Mol. Biomol. Spectrosc. (2020), https://doi.org/10.1016/j.saa.2020.118303.

[3] A. Sosna-Głębska, N. Szczecińska, K. Znajdek, M. Sibiński, Review on metallic oxide nanoparticles and their application in optoelectronic devices, Acta Innovat. (2019), https://doi.org/10.32933/ActaInnovations.30.1.

[4] D. Ouyang, Z. Huang, W.C. Choy, Solution-processed metal oxide nanocrystals as carrier transport layers in organic and perovskite solar cells, Adv. Funct. Mater. (2019), https://doi.org/10.1002/adfm.201804660.

[5] M. Zhao, H.J. Peng, Z.W. Zhang, B.Q. Li, X. Chen, J. Xie, X. Chen, J.Y. Wei, Q. Zhang, J.Q. Huang, Activating inert metallic compounds for high-rate lithium-sulfur batteries through in situ etching of extrinsic metal, Angew. Chem. Int. Ed. (2019), https://doi.org/10.1002/anie.201812062.

[6] K.H. Al-Attiyah, A. Hashim, S.F. Obaid, Fabrication of novel (carboxy methyl cellulose–polyvinylpyrrolidone–polyvinyl alcohol)/lead oxide nanoparticles: structural and optical properties for gamma rays shielding applications, Int. J. Plast. Technol. (2019), https://doi.org/10.1007/s12588-019-09228-5.

[7] H. Karami, M.A. Karimi, S. Haghdar, A. Sadeghi, R. Mir-Ghasemi, S. Mahdi-Khani, Synthesis of lead oxide nanoparticles by sonochemical method and its application as cathode and anode of lead-acid batteries, Mater. Chem. Phys. (2008), https://doi.org/10.1016/j.matchemphys.2007.09.045.

[8] X. Sun, J. Yang, W. Zhang, X. Zhu, Y. Hu, D. Yang, X. Yuan, W. Yu, J. Dong, H. Wang, L. Li, Lead acetate trihydrate precursor route to synthesize novel ultrafine lead oxide from spent lead acid battery pastes, J. Power Sour. (2014), https://doi.org/10.1016/j.jpowsour.2014.07.007.

[9] A. Kraft, L. Labusch, T. Ensslen, I. Dürr, J. Bartsch, M. Glatthaar, S. Glunz, H. Reinecke, Investigation of acetic acid corrosion impact on printed solar cell contacts, IEEE J. Photovol. (2015), https://doi.org/10.1109/JPHOTOV.2015.2395146.

[10] D.K. Gaikwad, S.S. Obaid, M.I. Sayyed, R.R. Bhosale, V.V. Awasarmol, A. Kumar, M.D. Shirsat, P.P. Pawar, Comparative study of gamma ray shielding competence of WO_3-TeO_2-PbO glass system to different glasses and concretes, Mater. Chem. Phys. (2018), https://doi.org/10.1016/j.matchemphys.2018.04.019.

[11] M.M. Kashani-Motlagh, M.K. Mahmoudabad, Synthesis and characterization of lead oxide nano-powders by sol–gel method, J. Sol-Gel Sci. Technol. (2011), https://doi.org/10.1007/s10971-011-2467-y.

[12] S.K. Pasha, K. Deshmukh, M.B. Ahamed, K. Chidambaram, M.K. Mohanapriya, N.A. N. Raj, Investigation of microstructure, morphology, mechanical, and dielectric properties of PVA/PbO nanocomposites, Adv. Polym. Tech. (2017), https://doi.org/10.1002/adv.21616.

[13] M. Salavati-Niasari, F. Mohandes, F. Davar, Preparation of PbO nanocrystals via decomposition of lead oxalate, Polyhedron (2009), https://doi.org/10.1016/j.poly.2009.04.009.

[14] L. Esrafili, A.A. Tehrani, A. Morsali, L. Carlucci, D.M. Proserpio, Ultrasound and solvothermal synthesis of a new urea-based metal-organic framework as a precursor for fabrication of cadmium (II) oxide nanostructures, Inorg. Chim. Acta (2019), https://doi.org/10.1016/j.ica.2018.09.025.

[15] M.J.S. Fard, P. Hayati, A. Firoozadeh, J. Janczak, Ultrasonic synthesis of two new zinc (II) bipyridine coordination nano-particles polymers: new precursors for preparation of zinc (II) oxide nano-particles, Ultrason. Sonochem. (2017), https://doi.org/10.1016/j.ultsonch.2016.11.009.

[16] H. Karami, M.A. Karimi, S. Haghdar, Synthesis of uniform nano-structured lead oxide by sonochemical method and its application as cathode and anode of lead-acid batteries, Mater. Res. Bull. (2008), https://doi.org/10.1016/j.materresbull.2007.11.014.

[17] Q. Li, C. Feng, Electrochemical performance of nanostructured PbO@C obtained by sol-gel method, J. Electron. Mater. (2016), https://doi.org/10.1007/s11664-016-4411-y.

[18] D.P. Singh, O.N. Srivastava, Synthesis of micron-sized hexagonal and flower-like nanostructures of lead oxide (PbO_2) by anodic oxidation of lead, Nano-Micro Lett. (2011), https://doi.org/10.1007/BF03353676.

[19] S.H. Ng J. Wang K. Konstantinov D. Wexler J. Chen H.K. Liu Spray pyrolyzed PbO-carbon nanocomposites as anode for lithium-ion batteries Journal of The Electrochemical Society. 2006 http://ro.uow.edu.au/engpapers/101.

[20] C.G. Poll, D.J. Payne, Electrochemical synthesis of PbO_2, Pb_3O_4 and PbO films on a transparent conducting substrate, Electrochim. Acta (2015), https://doi.org/10.1016/j.electacta.2015.01.019.

[21] H. Sivaram, D. Selvakumar, A. Alsalme, A. Alswieleh, R. Jayavel, Enhanced performance of PbO nanoparticles and PbO-CdO and PbO-ZnO nanocomposites for supercapacitor application, J. Alloy. Compd. (2018), https://doi.org/10.1016/j.jallcom.2017.10.025.

[22] B. Jia, L. Gao, Synthesis and characterization of single crystalline PbO nanorods via a facile hydrothermal method, Mater. Chem. Phys. (2006), https://doi.org/10.1016/j.matchemphys.2006.01.012.

[23] F. Behnoudnia, H. Dehghani, Synthesis and characterization of novel three-dimensional-cauliflower-like nanostructure of lead (II) oxalate and its thermal decomposition for preparation of PbO, Inorg. Chem. Commun. (2012), https://doi.org/10.1016/j.inoche.2012.07.031.

[24] R.S. Yadav, I. Kuřitka, J. Vilcakova, J. Havlica, L. Kalina, P. Urbánek, M. Machovsky, D. Skoda, M. Masař, M. Holek, Sonochemical synthesis of Gd_3+ doped $CoFe_2O_4$ spinel ferrite nanoparticles and its physical properties, Ultrason. Sonochem. (2018), https://doi.org/10.1016/j.ultsonch.2017.08.024.

[25] J. Zhu, Y. Koltypin, A. Gedanken, General sonochemical method for the preparation of nanophasic selenides: synthesis of ZnSe nanoparticles, Chem. Mater. (2000), https://doi.org/10.1021/cm990380r.

[26] J.J. Zhu, H. Wang, S. Xu, H.Y. Chen, Sonochemical method for the preparation of monodisperse spherical and rectangular lead selenide nanoparticles, Langmuir (2002), https://doi.org/10.1021/la010988q.

[27] J. Zhu, S. Liu, O. Palchik, Y. Koltypin, A. Gedanken, A novel sonochemical method for the preparation of nanophasic sulfides: synthesis of HgS and PbS nanoparticles, J. Solid State Chem. (2000), https://doi.org/10.1006/jssc.2000.8780.

[28] A. Gedanken, Using sonochemistry for the fabrication of nanomaterials, Ultrason. Sonochem. (2004), https://doi.org/10.1016/j.ultsonch.2004.01.037.

[29] F. Foroughi, J.J. Lamb, O.S. Burheim, B.G. Pollet, Sonochemical and sonoelectrochemical production of energy materials, Catalysts (2021), https://doi.org/10.3390/catal11020284.

[30] B. Mirtamizdoust, Z. Trávníček, Y. Hanifehpour, P. Talemi, H. Hammud, S.W. Joo, Synthesis and characterization of nano-peanuts of lead (II) coordination polymer $[Pb\ (qcnh)(NO_3)_2]_n$ with ultrasonic assistance: a new precursor for the preparation of pure-phase nano-sized PbO, Ultrason. Sonochem. (2017), https://doi.org/10.1016/j.ultsonch.2016.05.041.

[31] S.D. Ayare, P.R. Gogate, Sonocatalytic treatment of phosphonate containing industrial wastewater intensified using combined oxidation approaches, Ultrason. Sonochem. (2019), https://doi.org/10.1016/j.ultsonch.2018.10.018.

[32] İ. Deveci, B. Mercimek, Performance of SiO_2/Ag Core/Shell particles in sonocatalalytic degradation of Rhodamine B, Ultrason. Sonochem. (2019), https://doi.org/10.1016/j.ultsonch.2018.10.025.

[33] Y. Sun, M. Zhang, D. Fan, Effect of ultrasonic on deterioration of oil in microwave vacuum frying and prediction of frying oil quality based on low field nuclear magnetic resonance (LF-NMR), Ultrason. Sonochem. (2019), https://doi.org/10.1016/j.ultsonch.2018.10.015.

[34] J. Theerthagiri, J. Madhavan, S.J. Lee, M.Y. Choi, M. Ashokkumar, B.G. Pollet, Sonoelectrochemistry for energy and environmental applications, Ultrason. Sonochem. (2020), https://doi.org/10.1016/j.ultsonch.2020.104960.

[35] F. Arab, M. Mousavi-Kamazani, M. Salavati-Niasari, Facile sonochemical synthesis of tellurium and tellurium dioxide nanoparticles: Reducing Te (IV) to Te via ultrasonic irradiation in methanol, Ultrason. Sonochem. (2017), https://doi.org/10.1016/j.ultsonch.2017.01.026.

[36] F. Mohandes, M. Salavati-Niasari, Sonochemical synthesis of silver vanadium oxide micro/nanorods: solvent and surfactant effects, Ultrason. Sonochem. (2013), https://doi.org/10.1016/j.ultsonch.2012.05.002.

[37] C. Pétrier, A. Francony, Ultrasonic waste-water treatment: incidence of ultrasonic frequency on the rate of phenol and carbon tetrachloride degradation, Ultrason. Sonochem. (1997), https://doi.org/10.1016/S1350-4177(97)00036-9.

[38] S.Y. Darki, M. Eslami-Kalantari, H. Zare, Z. Shahedi, Effects of PVP surfactant and different alkalis on the properties of PbO nanostructures, Mater. Chem. Phys. (2021), https://doi.org/10.1016/j.matchemphys.2021.124305.

[39] S. Ghasemi, M.F. Mousavi, M. Shamsipur, H. Karami, Sonochemical-assisted synthesis of nano-structured lead dioxide, Ultrason. Sonochem. (2008), https://doi.org/10.1016/j.ultsonch.2007.05.006.

[40] U.K. Bangi, H.H. Park, W. Han, V.M. Prakshale, L.P. Deshmukh, Ultrasonically assisted synthesis of lead oxide nanoflowers using ball milling, Int. Nano Lett. (2017), https://doi.org/10.1007/s40089-017-0209-z.

[41] M. Mahdiani, F. Soofivand, M. Salavati-Niasari, Investigation of experimental and instrumental parameters on properties of $PbFe_{12}O_{19}$ nanostructures prepared by sonochemical method, Ultrason. Sonochem. (2018), https://doi.org/10.1016/j.ultsonch.2017.06.023.

[42] S. Mustapha, M.M. Ndamitso, A.S. Abdulkareem, J.O. Tijani, D.T. Shuaib, A. K. Mohammed, A. Sumaila, Comparative study of crystallite size using Williamson-Hall and Debye-Scherrer plots for ZnO nanoparticles, Adv. Nat. Sci. Nanosci. Nanotechnol. (2019), https://doi.org/10.1088/2043-6254/ab52f7.

[43] Y. Borodko, S.E. Habas, M. Koebel, P. Yang, H. Frei, G.A. Somorjai, Probing the interaction of poly (vinylpyrrolidone) with platinum nanocrystals by UV-Raman and FTIR, J. Phys. Chem. B (2006), https://doi.org/10.1021/jp063338+.

[44] N. Tanaka, K. Ito, H. Kitano, Raman spectroscopic study of hydrogen bonding of poly (N-vinyl-2-pyrrolidone) in heavy water and dimethyl sulfoxide, Macromol. Chem. Phys. (1994), https://doi.org/10.1002/macp.1994.021951008.

[45] I.A. Safo, C. Dosche, M. Oezaslan, TEM, FTIR and electrochemistry study: desorption of PVP from Pt nanocubes, Z. Phys. Chem. (2018), https://doi.org/10.1515/zpch-2018-1147.